Laser Physics, Vol. 12, No. 12, 2002, pp. 1402–1409.

Resonant Three-Photon Ionization of Atomic Hydrogen in a Finite-Bandwidth Laser Field and a Static Electric Field

B. J. Shortt[1,*], P. J. M. van der Burgt[1], and F. Giammanco[2]

[1] *Department of Experimental Physics, National University of Ireland, Maynooth, Co. Kildare, Ireland*
[2] *Instituto Nazionale di Fisica della Materia e Dipartimento di Fisica, Università di Pisa, Pisa, 56126 Italy*
e-mail: giamma@df.unipi.it

Received March 6, 2002

Abstract—We derive a set of density matrix equations describing laser photo-excitation and ionization of atomic hydrogen in the presence of an external electric field. The equations are relevant as a description of multiphoton ionization of hydrogen (or deuterium) atoms in laser-produced transient plasmas. The laser wavelength is 243 nm, so that the photoionization is resonant with the $2s_{1/2}$ level. The electric field causes Stark mixing of the $2s_{1/2}$ level with the $2p_{1/2}$ and $2p_{3/2}$ levels. Because the electric field is taken in the same direction as the linear polarization of the laser, only states with equal m_j are coupled, and the atom can be described with a four-level density matrix. The laser bandwidth is taken into account by using the stochastic model of a chaotic laser field introduced by Zoller [1]. We present a few calculations of the probabilities for ionization and excitation of a single hydrogen atom as a function of laser intensity and wavelength.

1. INTRODUCTION

When a pulsed laser beam is focussed into a low-pressure gas of atoms, a large number of photo-electrons and ions may be generated by multiphoton ionization of the atoms in the gas. During and shortly after the laser pulse collective effects depending on the mutual interaction of the photo-electrons and the ions in the transient plasma affect the spatial and temporal distribution of both charged species. In an ongoing research programme [2] we investigate the collective effects in transient non-equilibrium plasmas produced by three-photon ionization of deuterium atoms with a pulsed laser beam. In the experiment the laser wavelength is tuned to 243 nm, so that the photoionization is resonant with the metastable $2s_{1/2}$ state. The ion yield, the ion time-of-flight spectra and the yield of metastable atoms are measured as a function of the laser intensity, the laser wavelength, and the target density. During and shortly after the laser pulse collective effects depending on the mutual interaction of the electrons and the ions affect the spatial and temporal distribution of the ions. As a result the time-dependent yields of ions and of metastable atoms are modulated by the interplay of two processes: (i) the multiphoton ionization of the atoms, and (ii) the collective effects in the plasma. Multiphoton ionization of deuterium presents an ideal situation for the study of this interplay. Deuterium is almost the lightest element and therefore deuterium ions are very susceptible to the collective field, and the near-degeneracy of the $2s_{1/2}$, $2p_{1/2}$ and $2p_{3/2}$ states makes that the resonant multiphoton ionization is affected by the Stark mixing of these states in the collective field.

In order to be able to model the time evolution of the transient plasma one needs to include a description of the production of photo-electrons and ions by photoionization during the laser pulse. The collective model used by Bowe *et al.* [2], which is based on a fluid-dynamics description of the coupled motion of the ions and electrons based on the Boltzmann transport equations [3], incorporates two-level rate equations to describe the photoionization process. In this paper we develop an improved description of the photoionization process by using a four-level density matrix description. The four-level density matrix describes a hydrogen atom in a chaotic finite-bandwidth laser field and a static electric field, and can be used in the modelling of transient plasmas as a function of the laser detuning around the $1s$–$2s$ resonance. In the collective model an array of density matrices will be needed to represent the interaction region and to allow for temporal and spatial variations of the collective electric field across the interaction region. New fluid-dynamics calculations will be compared with new experimental results in a future paper. The purpose of this paper is to discuss the density matrix description and to present several calculations for the photoionization of a single hydrogen atom. Because of the close similarity of the electronic wavefunctions of hydrogen and deuterium the density matrix equations are applicable to deuterium as well.

As discussed by Holt *et al.* [4] and Dörr *et al.* [5] multiphoton ionization of an atom with one intermediate resonant state may be modelled as a two-level system with a time-independent 2×2 Hamiltonian. If the

* Present address: Atomic and Molecular Collisions Team, MS 121-104, Jet Propulsion Laboratory, 4800 Oak Grove Drive, Pasadena, CA 91109-8099, USA

matrix elements of the Hamiltonian are known as a function of intensity and laser frequency, then ionization rates and population probabilities are obtained by solving the time-dependent Schrödinger equation for the wavefunction or the Liouville equation for the density matrix. Holt *et al.* [4] have calculated the two-level Hamiltonian matrix elements for multiphoton ionization of hydrogen using a generalized Floquet formulation. Dörr *et al.* [5] have shown that for resonant two-photon coupling of the hydrogen $1s_{1/2}$ and $2s_{1/2}$ states, a 2×2 effective Hamiltonian reproduces to satisfactory accuracy the solution of the full Schrödinger equation.

The purpose of this paper is to apply the density matrix formalism to three-photon resonant ionization of atomic hydrogen and to extend it in two ways. Firstly, in order to describe Stark mixing of the resonant $2s_{1/2}$ level with the adjacent $2p_{1/2}$ and $2p_{3/2}$ levels in an external static electric field, we use a four-level description with a 4×4 effective Hamiltonian. Conform our experimental set-up, we assume that the laser beam is fully 100% linearly polarized and that the linear polarization is in the same direction as the static electric field. Under these circumstances only levels with equal m_j, are coupled, and a four-level description is adequate. In case the electric field would not be aligned with the laser polarization all m_j levels would have to be included, resulting in a 10-level description.

Secondly, we include a realistic description of the finite laser bandwidth. Two particular stochastic models have been well studied (see Georges and Lambropoulos [6] and references therein). The phase diffusion model describes the field of an intensity-stabilized cw laser, which has only phase fluctuations. The chaotic field model describes the field of a pulsed multimode laser which has fluctuations in both phase and amplitude. In this paper we adopt the stochastic model for a chaotic laser field introduced by Zoller [1]. In this model the system of stochastic differential equations for the density matrix elements is reduced to a tractable infinite set of differential equations. For a given laser bandwidth, this set of equations can be truncated and numerically integrated. For large laser bandwidths the zero-order set of equations already gives quite good results.

The effects of finite laser bandwidth on two-photon resonant three-photon ionization of sodium atoms have been studied by several groups. Agostini *et al.* [7] present measurements of the ion yield as a function of laser intensity for two different laser bandwidths. They also derive two-level density matrix equations assuming that the populations of the atomic levels can be decorrelated from the field variables. Zoller and Lambropoulos [8] have applied the chaotic field model of Zoller [1] to a two-level density matrix description of multiphoton ionization of sodium. They compare calculations of the ionization probability for a chaotic field with calculations using a phase diffusion model. In this paper we extend the model of Zoller [1] to a four-level density matrix description of multiphoton ionization of hydrogen.

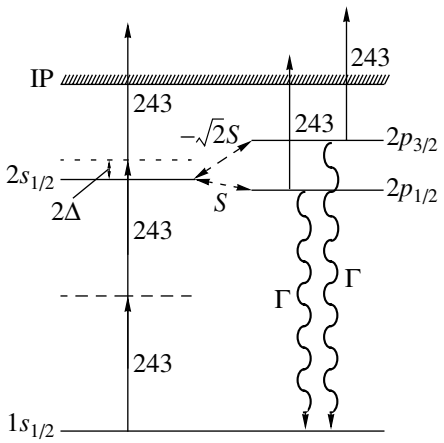

Fig. 1. Energy level diagram.

2. THEORY

2.1. A Hydrogen Atom in a Monochromatic Laser Field and a Static Electric Field

The four atom + field eigenstates used as basis states are:

$$\begin{aligned} |1\rangle &= |1s_{1/2}, m_j = 1/2, \bar{n}\rangle, \\ |2\rangle &= |2p_{1/2}, m_j = 1/2, \bar{n} - 2\rangle, \\ |3\rangle &= |2s_{1/2}, m_j = 1/2, \bar{n} - 2\rangle, \\ |4\rangle &= |2p_{3/2}, m_j = 1/2, \bar{n} - 2\rangle, \end{aligned} \tag{1}$$

where $\bar{n}$ is the average number of 243 nm photons in the field. We only consider states with $m_j = 1/2$, because the linear polarization of the laser and the static electric field are taken to be in the same direction, along the z-axis, and they do not couple states with different m_j. The laser field causes a two-photon coupling of the states $|1\rangle$ and $|3\rangle$, and the static electric field causes Stark mixing of the states $|2\rangle$, $|3\rangle$, and $|4\rangle$. The couplings are illustrated in Fig. 1. On this basis of eigenstates, the 4×4 Hamiltonian matrix has the diagonal elements:

$$\begin{aligned} H_{11} &= E_1 + \delta_1 = \delta_1, \\ H_{22} &= E_2 - 2\hbar\omega + \delta_2 = E_2 - E_3 - 2\Delta + \delta_2, \\ H_{33} &= E_3 - 2\hbar\omega + \delta_3 = -2\Delta + \delta_3, \\ H_{44} &= E_4 - 2\hbar\omega + \delta_4 = E_4 - E_3 - 2\Delta + \delta_4, \end{aligned} \tag{2}$$

I is the laser intensity, $\Delta = \hbar\omega - E_3/2$ is the laser detuning (single-photon detuning), and δ_1, δ_2, δ_3, and δ_4 are the ac Stark shifts. Because the $1s$–$2s$ two-photon coupling is included in our model as an off-diagonal matrix element, δ_1 and δ_3 are the ac Stark shifts due to all hydrogen states other than the $1s$ and $2s$ states, whereas δ_2 and δ_4 include contributions from all states.

The non-zero off-diagonal elements of the Hamiltonian matrix are:

$$H_{13} = H_{31}^{*} = \frac{1}{2}\Omega e^{2i\varphi},$$
$$H_{23} = H_{32} = S, \tag{3}$$
$$H_{34} = H_{43} = -\sqrt{2}S$$

with

$$S = \sqrt{3}ea_0E, \tag{4}$$

E is the static electric field in the interaction region, Ω is the Rabi frequency for the two-photon coupling of the states $|1\rangle$ and $|3\rangle$, and φ is the phase of the laser field. E can be interpreted either as an external electric field, or as the collective field generated by a laser-produced plasma. E could be slowly varying in time but in this paper is taken to be constant during the laser pulse. It is assumed that the laser light is monochromatic and 100% linearly polarized, and the polarization direction coincides with the direction of the static electric field.

Loss due to photoionization and Lyman-α radiative decay is described by introducing the diagonal matrix:

$$G = \begin{pmatrix} 0 & 0 & 0 & 0 \\ 0 & \gamma_2 + \Gamma & 0 & 0 \\ 0 & 0 & \gamma_3 & 0 \\ 0 & 0 & 0 & \gamma_4 + \Gamma \end{pmatrix}, \tag{5}$$

where Γ is the inverse lifetime of the $2p_{1/2}$ and $2p_{3/2}$ states, and γ_2, γ_3, and γ_4 are the ionization widths of the states $|2\rangle$, $|3\rangle$, and $|4\rangle$.

Using both the Hamiltonian matrix H and the loss matrix G, the Liouville equation for the slowly-varying density matrix ρ becomes [9]:

$$\frac{d\rho}{dt} = \frac{1}{i\hbar}[H, \rho] - \frac{1}{2}(G\rho + \rho G) + \text{spontaneous decay term}. \tag{6}$$

The spontaneous decay term is $\Gamma(\rho_{22} + \rho_{44})$; it only enters the equation for ρ_{11} and describes the incoherent increase in population of the ground state $|1\rangle$ due to the spontaneous decay of the excited states $|2\rangle$ and $|4\rangle$.

This equation can also be written in the form

$$\left(i\frac{d}{dt} + \overleftrightarrow{Q}(I(t), \varphi(t))\right)\boldsymbol{\rho}(t) = 0, \tag{7}$$

where $\boldsymbol{\rho}$ is a column vector of the density matrix elements and $\overleftrightarrow{Q}$ is a 16×16 matrix. The equations for the individual density matrix elements are

$$\frac{d\rho_{11}}{dt} = \Gamma(\rho_{22} + \rho_{44}) - i\frac{1}{2}\Omega(e^{2i\varphi}\rho_{31} - e^{-2i\varphi}\rho_{13}),$$

$$\frac{d\rho_{22}}{dt} = -(\Gamma + \gamma_2)\rho_{22} - 2S\,\mathrm{Im}(\rho_{23}),$$

$$\frac{d\rho_{33}}{dt} = -\gamma_3\rho_{33} + i\frac{1}{2}\Omega(e^{2i\varphi}\rho_{31} - e^{-2i\varphi}\rho_{13}) + 2S\,\mathrm{Im}(\rho_{23}) + 2\sqrt{2}S\,\mathrm{Im}(\rho_{34}),$$

$$\frac{d\rho_{44}}{dt} = -(\Gamma + \gamma_4)\rho_{44} - 2\sqrt{2}S\,\mathrm{Im}(\rho_{34}),$$

$$\frac{d\rho_{12}}{dt} = \left[-\frac{1}{2}(\Gamma + \gamma_2) + i(E_2 - E_3 - 2\Delta + \delta_2 - \delta_1)\right]\rho_{12} - i\frac{1}{2}\Omega e^{2i\varphi}\rho_{32} + iS\rho_{13},$$

$$\frac{d\rho_{13}}{dt} = \left[-\frac{1}{2}\gamma_3 + i(-2\Delta + \delta_3 - \delta_1)\right]\rho_{13} + i\frac{1}{2}\Omega e^{2i\varphi}(\rho_{11} - \rho_{33}) + iS\rho_{12} - i\sqrt{2}S\rho_{14}, \tag{8}$$

$$\frac{d\rho_{14}}{dt} = \left[-\frac{1}{2}(\Gamma + \gamma_4) + i(E_4 - E_3 - 2\Delta + \delta_4 - \delta_1)\right]\rho_{14} - i\frac{1}{2}\Omega e^{2i\varphi}\rho_{34} - i\sqrt{2}S\rho_{13},$$

$$\frac{d\rho_{23}}{dt} = \left[-\frac{1}{2}(\Gamma + \gamma_2 + \gamma_3) + i(E_3 - E_2 + \delta_3 - \delta_2)\right]\rho_{23} + i\frac{1}{2}\Omega e^{2i\varphi}\rho_{21} + iS(\rho_{22} - \rho_{33}) - i\sqrt{2}S\rho_{24},$$

$$\frac{d\rho_{24}}{dt} = \left[-\left(\Gamma + \frac{1}{2}\gamma_2 + \frac{1}{2}\gamma_4\right) + i(E_4 - E_2 + \delta_4 - \delta_2)\right]\rho_{24} - iS\rho_{34} - i\sqrt{2}S\rho_{23},$$

$$\frac{d\rho_{34}}{dt} = \left[-\frac{1}{2}(\Gamma + \gamma_3 + \gamma_4) + i(E_4 - E_3 + \delta_4 - \delta_3)\right]\rho_{34} - i\frac{1}{2}\Omega e^{-2i\varphi}\rho_{14} - iS\rho_{24} - i\sqrt{2}S(\rho_{33} - \rho_{44}).$$

The equations for the elements in the lower-left corner of the density matrix are easily obtained using $\rho_{ji} = \rho_{ij}^{*}$.

2.2. A Hydrogen Atom in a Finite-Bandwidth Chaotic Laser Field and a Static Electric Field

According to the formalism discussed by Zoller [1], the average populations of the atomic levels can be found using the system of partial differential equations:

$$\left[i\left(\frac{d}{dt} + L\right) + \overleftrightarrow{Q}(I, \varphi)\right]\boldsymbol{\rho}(I, \varphi, t) = 0, \tag{9}$$

where L is the Fokker–Planck operator. This system of equations can be solved by expanding each element of the column vector $\boldsymbol{\rho}$ as

$$\rho_{ij}(I, \varphi, t) = \sum_{\alpha n} P_{\alpha n}(I, \varphi)\rho_{ij}^{\alpha n}(t) \tag{10}$$

with

$$\rho_{ij}^{\alpha n}(t) = \int_0^\infty \varphi_{\alpha n}^*(I, \varphi)\rho_{ij}(I, \varphi, t)dId\varphi. \tag{11}$$

In these equations $\varphi_{\alpha n}(I, \varphi)$ and $P_{\alpha n}(I, \varphi)$ are eigenfunctions of L, as given in [1]. By inserting Eq. (10) into Eq. (9) we obtain an infinite set of differential equations for the unknown coefficients $\rho_{ij}^{\alpha n}(t)$. If we use the initial condition

$$\rho_{ij}^{\alpha n}(t=0) = \delta_{i0}\delta_{j0}\delta_{\alpha 0}\delta_{n0}, \tag{12}$$

we obtain the following set of equations:

$$\left(\frac{d}{dt} + \Lambda_{0n}\right)\rho_{11}^{0n} = \Gamma(\rho_{22}^{0n} + \rho_{44}^{0n})$$

$$- i\frac{1}{2}\Omega\sum_m [(0n|-2m)\rho_{31}^{-2m} - (0n|2m)\rho_{13}^{2m}],$$

$$\left(\frac{d}{dt} + \Lambda_{0n}\right)\rho_{22}^{0n}$$

$$= -\Gamma\rho_{22}^{0n} - \gamma_2\sum_m (0n|0m)\rho_{22}^{0m} - 2S\,\mathrm{Im}(\rho_{23}^{0n}),$$

$$\left(\frac{d}{dt} + \Lambda_{0n}\right)\rho_{33}^{0n} = -\gamma_3\sum_m (0n|0m)\rho_{33}^{0m}$$

$$+ i\frac{1}{2}\Omega\sum_m [(0n|-2m)\rho_{31}^{-2m} - (0n|2m)\rho_{13}^{2m}]$$

$$+ 2S\,\mathrm{Im}(\rho_{23}^{0n}) + 2\sqrt{2}S\,\mathrm{Im}(\rho_{34}^{0n}),$$

$$\left(\frac{d}{dt} + \Lambda_{0n}\right)\rho_{44}^{0n}$$

$$= -\Gamma\rho_{44}^{0n} - \gamma_4\sum_m (0n|0m)\rho_{44}^{0n} - 2\sqrt{2}S\,\mathrm{Im}(\rho_{34}^{0n}),$$

$$\left(\frac{d}{dt} + \Lambda_{2n}\right)\rho_{12}^{2n} = \left[-\frac{1}{2}\Gamma + i(E_2 - E_3 - 2\Delta)\right]\rho_{12}^{2n}$$

$$+ \left(-\frac{1}{2}\gamma_2 + i\delta_2 - i\delta_1\right)\sum_m (2n|2m)\rho_{12}^{2m}$$

$$- i\frac{1}{2}\Omega\sum_m (2n|0m)\rho_{32}^{0m} + iS\rho_{13}^{2n},$$

$$\left(\frac{d}{dt} + \Lambda_{2n}\right)\rho_{13}^{2n} = -2i\Delta\rho_{13}^{2n} + \left(-\frac{1}{2}\gamma_3 + i\delta_3 - i\delta_1\right)$$

$$\times\sum_m (2n|2m)\rho_{13}^{2m} + i\frac{1}{2}\Omega\sum_m (2n|0m)(\rho_{11}^{0m} - \rho_{33}^{0m}) \tag{13}$$

$$+ iS\rho_{12}^{2n} - i\sqrt{2}S\rho_{14}^{2n},$$

$$\left(\frac{d}{dt} + \Lambda_{2n}\right)\rho_{14}^{2n} = \left[-\frac{1}{2}\Gamma + i(E_4 - E_3 - 2\Delta)\right]\rho_{14}^{2n}$$

$$+ \left(-\frac{1}{2}\gamma_4 + i\delta_4 - i\delta_1\right)\sum_m (2n|2m)\rho_{14}^{2m}$$

$$- i\frac{1}{2}\Omega\sum_m (2n|0m)\rho_{34}^{0m} - i\sqrt{2}S\rho_{13}^{2n},$$

$$\left(\frac{d}{dt} + \Lambda_{0n}\right)\rho_{23}^{0n} = \left[-\frac{1}{2}\Gamma + i(E_3 - E_2)\right]\rho_{23}^{0n}$$

$$+ \left(-\frac{1}{2}\gamma_2 - \frac{1}{2}\gamma_3 + i\delta_3 - i\delta_2\right)\sum_m (0n|0m)\rho_{23}^{0m}$$

$$+ i\frac{1}{2}\Omega\sum_m (0n|-2m)\rho_{21}^{-2m} + iS(\rho_{22}^{0n} - \rho_{33}^{0n}) - i\sqrt{2}S\rho_{24}^{0n},$$

$$\left(\frac{d}{dt} + \Lambda_{0n}\right)\rho_{24}^{0n} = [-\Gamma + i(E_4 - E_2)]\rho_{24}^{0n}$$

$$+ \left(-\frac{1}{2}\gamma_2 - \frac{1}{2}\gamma_4 + i\delta_4 - i\delta_2\right)\sum_m (0n|0m)\rho_{24}^{0m}$$

$$- iS\rho_{34}^{0n} - i\sqrt{2}S\rho_{23}^{0n},$$

$$\left(\frac{d}{dt} + \Lambda_{0n}\right)\rho_{34}^{0n} = \left[-\frac{1}{2}\Gamma + i(E_4 - E_3)\right]\rho_{34}^{0n}$$

$$+ \left(-\frac{1}{2}\gamma_3 - \frac{1}{2}\gamma_4 + i\delta_4 - i\delta_3\right)\sum_m (0n|0m)\rho_{34}^{0m}$$

$$- i\frac{1}{2}\Omega\sum_m (0n|2m)\rho_{14}^{2m} - iS\rho_{24}^{0n} - i\sqrt{2}S(\rho_{33}^{0n} - \rho_{44}^{0n}).$$

In these equations $\Lambda_{\alpha n} = \gamma_L\left(n + \frac{1}{2}|\alpha|\right)$ where γ_L the bandwidth of the laser. The matrix elements are defined $(\alpha n|\beta m) \equiv \int_0^\infty \varphi_{\alpha n}(I) I P_{\beta m}(I) dI$, with the functions $\varphi_{\alpha n}(I)$ and $P_{\beta m}(I)$ as given in [1]. The matrix elements used in the equations above are

$$\begin{aligned}
(0n|0m) &= (2n+1)\delta_{nm} - (n+1)\delta_{n,m-1} - n\delta_{n,m+1},\\
(2n|2m) &= (2n+3)\delta_{nm}\\
&\quad - \sqrt{(n+1)(n+3)}\,\delta_{n,m-1} - \sqrt{n(n+2)}\,\delta_{n,m+1},\\
(0n|\pm 2m) &= \sqrt{(n+1)(n+2)}\,\delta_{nm}\\
&\quad - 2\sqrt{n(n+1)}\,\delta_{n,m+1} + \sqrt{(n-1)n}\,\delta_{n,m+2},\\
(\pm 2n|0m) &= \sqrt{(n+1)(n+2)}\,[\delta_{nm} - 2\delta_{n,m-1} + \delta_{n,m-2}].
\end{aligned} \tag{14}$$

The equations for the ρ_{21}^{-2n}, ρ_{31}^{-2n}, ρ_{41}^{-2n}, ρ_{32}^{0n}, ρ_{42}^{0n}, and ρ_{43}^{0n} elements can be obtained by using $\rho_{ji}^{-\alpha n} = (\rho_{ij}^{\alpha n})^*$. Solving this set of equations the average populations of the atomic levels are obtained from

$$\langle \rho_{ij}(t) \rangle = \rho_{ij}^{00}(t). \tag{15}$$

A zero-order set of equations is obtained by using $n = m = 0$, $\Lambda_{00} = 0$, and $\Lambda_{20} = \gamma_L$. If we simplify the notation by writing $\rho_{ij} \equiv \rho_{ij}^{00}$, and introduce new elements $\rho_{12} \equiv \sqrt{2}\rho_{12}^{20}$, $\rho_{13} \equiv \sqrt{2}\rho_{13}^{20}$, $\rho_{14} \equiv \sqrt{2}\rho_{14}^{20}$ most of the equations obtained are identical to Eqs. (8) with $\varphi = 0$. The only equations that change are:

$$\begin{aligned}
\frac{d\rho_{12}}{dt} &= \left[-\left(\gamma_L + \frac{1}{2}\Gamma + \frac{3}{2}\gamma_2\right)\right.\\
&\left. + i(E_2 - E_3 - 2\Delta + 3\delta_2 - 3\delta_1)\right]\rho_{12} - i\Omega\rho_{32} + iS\rho_{13},\\
\frac{d\rho_{13}}{dt} &= \left[-\left(\gamma_L + \frac{3}{2}\gamma_3\right) + i(-2\Delta + 3\delta_3 - 3\delta_1)\right]\rho_{13}\\
&\quad + i\Omega(\rho_{11} - \rho_{33}) + iS\rho_{12} - i\sqrt{2}S\rho_{14},\\
\frac{d\rho_{14}}{dt} &= \left[-\left(\gamma_L + \frac{1}{2}\Gamma + \frac{3}{2}\gamma_4\right)\right.\\
&\left. + i(E_4 - E_3 - 2\Delta + 3\delta_4 - 3\delta_1)\right]\rho_{14} - i\Omega\rho_{34} - i\sqrt{2}S\rho_{13}.
\end{aligned} \tag{16}$$

The subset of equations for ρ_{11}, ρ_{33}, and ρ_{13} are equivalent to the two-level-atom equations of Agostini *et al.* [7] and Dai and Lambropoulos [10]. The factors 3 appearing in front of δ_i and γ_i as well as the replacement of $\frac{1}{2}\Omega$ by Ω in the equations for ρ_{12}, ρ_{13}, and ρ_{14} have their origin in amplitude fluctuations; the presence of γ_L accounts for phase fluctuations.

2.3. Numerical Values for the Parameters

The sets of equations (8) and (13) can be evaluated numerically by using the following values for the parameters in the equations. The energy differences between the $n = 2$ states are $E_2 - E_3 = -1.0$ GHz and $E_4 - E_3 = 10.0$ GHz. Because the 1*s*–2*s* two-photon coupling is included in our model as an off-diagonal matrix element, δ_1 and δ_3 are the ac Stark shifts due to all hydrogen states other than the 1*s* and 2*s* states, whereas δ_2 and δ_4 include contributions from all states. Values of δ_1 and δ_3 as a function of laser intensity are obtained from [4]; values for δ_2 and δ_4 are obtained from Floquet calculations by Dörr [11]:

$$\begin{aligned}
\delta_1 &= (-1.68 \times 10^{-3})I \text{ GHz},\\
\delta_3 &= (8.81 \times 10^{-3})I \text{ GHz},\\
\delta_2 &= \delta_4 = (7.37 \times 10^{-3})I \text{ GHz},
\end{aligned} \tag{17}$$

where I is the laser intensity in MW/cm^2. Ω as a function of laser intensity is obtained from tabulated values in [4]:

$$\Omega = (4.60 \times 10^{-3})I \text{ GHz}. \tag{18}$$

γ_3 as a function of laser intensity is obtained from tabulated values in [4]; γ_2 and γ_4 are obtained from [11]:

$$\begin{aligned}
\gamma_3 &= (7.56 \times 10^{-3})I \text{ GHz},\\
\gamma_2 &= \gamma_4 = (5.93 \times 10^{-3})I \text{ GHz}.
\end{aligned} \tag{19}$$

The other relevant parameters are $\Gamma = 0.625$ GHz, and $S = (2.22 \times 10^{-3})E$ GHz, where E is the electric field strength in V/cm.

3. RESULTS AND DISCUSSION

In this section we compare our model with Floquet calculations, and we present a few calculations for photoionization of a hydrogen atom in the presence of a static electric field.

Dörr [11] has performed Floquet calculations for a hydrogen atom with 1*s*, 2*s*, and 2*p* basis states without fine structure, using the STRFLO code of Potvliege [12]. The calculations have been done for a laser wavelength of 243 nm ($\omega = 0.187503518$ a.u.). The results are listed in Table 1. As can be seen from the numbers in Table 1, the 2*p* state is perturbative over the range of laser intensities considered. Because the 1*s* and 2*s* states are resonantly coupled (there is a nearby complex-energy degeneracy, see Latinne *et al.* [13]), the shifts and widths for these states do not behave in a smooth manner. However, at low intensity both the shift and the width of the 1*s* and 2*s* states behave as expected, namely the shift is linear in intensity and the

width is proportional to I^n where n is the multiphoton ionization order ($n = 3$ for $1s$, $n = 1$ for $2s$).

In order to compare our model with Dörr's calculations we have set up a 3×3 complex Hamiltonian matrix using $1s$, $2s$, and $2p$ basis states without fine structure. The imaginary parts of the diagonal elements specify ionization rates in the laser field. The complex eigenvalues of this matrix need to be compared with Dörr's calculated complex energies. The only off-diagonal coupling in the 3×3 matrix due to the laser field is the $1s$–$2s$ coupling, and the complex energies E_{1s} and E_{2s} can be obtained by diagonalizing the 2×2 $1s$–$2s$ submatrix. The results are shown in Table 2, and are in good agreement with Dörr's results at lower laser intensities in Table 1. Because there are no off-diagonal $1s$–$2p$ and $2s$–$2p$ laser-couplings in our model (these couplings are included in the $2p$ ac Stark shift), our $2p$ diagonal term in the 3×3 matrix is exactly equal to E_{2p} from Dörr [11].

Comparison of Table 1 with Table 2 shows that perturbative calculations based on Eq. (8) for the 4-level hydrogen atom should yield accurate results for laser intensities below about 1000 MW/cm^2. We expect therefore that the finite bandwidth equations (Eq. (13)) provide a good first-order model for the multiphoton ionization of hydrogen and deuterium atoms in laser-produced transient plasmas.

We have implemented the sets of equations (8) and (13) into computer programs written in Fortran and in Delphi. These equations have been solved numerically using a fourth-order Runge–Kutta approximation with a time step of 0.01 ns. In a few cases a smaller time step of 0.0025 ns had to be chosen in order to obtain convergence. Results obtained with both programs were compared and found to be in agreement.

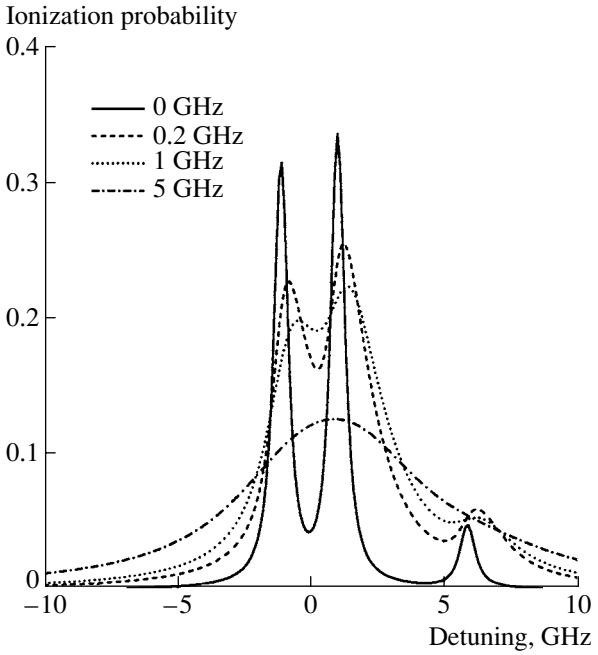

Fig. 2. Ionization probability as a function of laser detuning for a hydrogen atom in a laser field of 100 MW/cm^2 and a static electric field of 1000 V/cm. The laser has wavelength 243 nm and a Gaussian pulse of 13 ns. The curves for finite bandwidth are calculated using a 9th order expansion of equation (13). The curve for zero bandwidth is calculated using Eq. (8).

All calculations have been performed for a hydrogen atom in a laser field and a static electric field. Unless indicated otherwise, the laser field has intensity $I_0 = 100$ MW/cm^2, wavelength 243 nm, and bandwidth 0.2 GHz, and the static electric field strength is

Table 1. Floquet results [11]

I (MW/cm^2)	ReE_{1s} (a.u.)	ImE_{1s} (a.u.)	ReE_{2s} (a.u.)	ImE_{2s} (a.u.)	ReE_{2p} (a.u.)	ImE_{2p} (a.u.)
100	−0.50000002	-5.821×10^{-15}	−0.50000704	-9.134×10^{-9}	−0.50000702	-7.172×10^{-9}
300	−0.50000007	-1.593×10^{-13}	−0.50000703	-2.740×10^{-8}	−0.50000698	-2.152×10^{-8}
10^5	−0.50000469	-8.551×10^{-6}	−0.50002567	-5.836×10^{-7}	−0.49998922	-7.167×10^{-6}
10^6	−0.49998603	-8.768×10^{-5}	−0.50025420	-3.744×10^{-6}	−0.49982903	-7.125×10^{-5}
10^7	−0.49979352	-8.829×10^{-4}	−0.50253804	-3.880×10^{-5}	−0.49824501	-6.713×10^{-4}

Table 2. 2×2 diagonalization results

I (MW/cm^2)	ReE_{1s} (a.u.)	ImE_{1s} (a.u.)	ReE_{2s} (a.u.)	ImE_{2s} (a.u.)
100	−0.50000000	-5.722×10^{-15}	−0.50000701	-9.130×10^{-9}
300	−0.50000001	-1.567×10^{-13}	−0.50000697	-2.739×10^{-8}
10^5	−0.49998442	-8.556×10^{-6}	−0.50000539	-5.737×10^{-7}
10^6	−0.49978331	-8.765×10^{-5}	−0.50005142	-3.652×10^{-6}
10^7	−0.49777182	-8.779×10^{-4}	−0.50051221	-3.505×10^{-5}

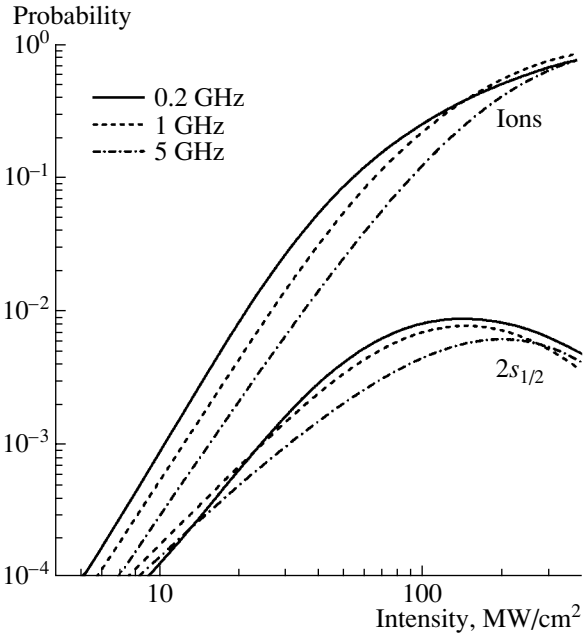

Fig. 3. Probabilities for ionization and $2s_{1/2}$-excitation as a function of laser intensity for a hydrogen atom in a static electric field of 1000 V/cm. The laser has wavelength 243 nm and a Gaussian pulse of 13 ns. The curves show the effect of the laser bandwidth on the probabilities. For each bandwidth the laser detuning is taken at the maximum of the middle peak in Fig. 2.

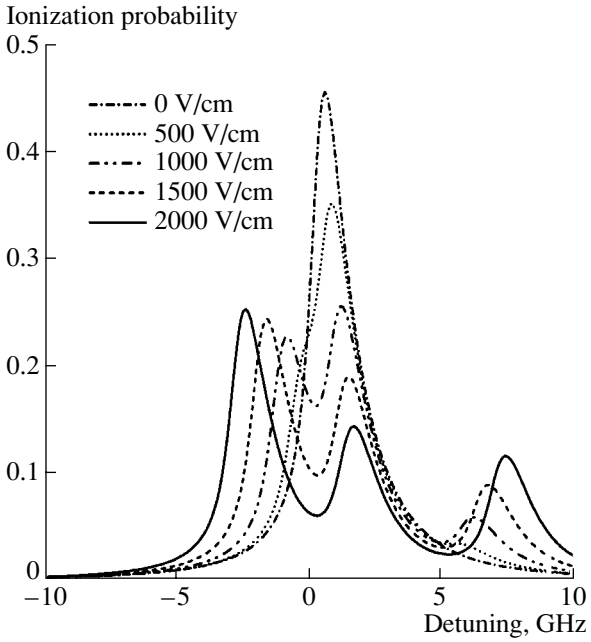

Fig. 4. Ionization probability as a function of laser detuning for a hydrogen atom in a laser field of intensity 100 MW/cm^2 and a static electric field of variable intensity. The laser has wavelength 243 nm, bandwidth 0.2 GHz, and a Gaussian pulse of 13 ns. The curves show the effect of the static electric field on the ionization probability.

1000 V/cm. The laser temporal profile is a Gaussian pulse $I(t) = I_0 \exp[-(2t/w - 1)^2]$, $t \in [0, w]$ with a pulse width $w = 13$ ns. All finite bandwidth calculations have been performed by evaluation of Eq. (13) up to 9th order.

Figure 2 shows the effect of the laser bandwidth on the ionization probability as a function of laser detuning. The mixed *s–p* character of each of the three Stark states is demonstrated by the fact that each Stark state acts as a resonant intermediate state in the photoionization. The laser bandwidth has a profound effect on the laser's ability to resolve the three atomic states. Notably, at a bandwidth of 5 GHz only a single peak is visible, with no indication of any structure in the line profile. The curves for finite bandwidth have been calculated using a 9th order expansion of Eq. (13). Even for the most narrow bandwidth of 0.2 GHz there is rapid convergence: there is very little difference between the 2nd order and the 9th order equations. For bandwidths of 5 GHz and higher the zero order equations provide a very good approximation.

Figure 3 shows the photoionization as a function of laser intensity for three different laser bandwidths. For each bandwidth the laser detuning is chosen at the maximum of the middle peak in Fig. 2: the detunings are 1.2, 1.4, and 0.90 GHz for bandwidths of 0.2, 1, and 5 GHz, respectively. All curves show an I^3 dependence at low intensities, as expected because in each case the probability of finding the hydrogen atom in the $2s_{1/2}$ state is much smaller than one. The probabilities for excitation of the $2s_{1/2}$ state only show an approximate I^2 dependence at low intensities, and reach a maximum between 100 and 200 MW/cm^2.

Figure 4 shows the ionization probability as a function of detuning for several values of the static electric field strength. As the electric field is increased photoionization via the $2p_{1/2}$ and $2p_{3/2}$ Stark states increases at the cost of photoionization via the $2s_{1/2}$ Stark state. The curves also illustrate the shifts in energy of the Stark-mixed states with increasing electric field strength. The peak positions are determined by both the dc Stark shifts due to the static electric field and the ac Stark shifts due to the laser field.

4. CONCLUSION

We have derived a set of density matrix equations describing photo-excitation and ionization of a hydrogen atom in a finite-bandwidth laser field and a static electric field. Our calculations show that due to the near-degeneracy of the $2s_{1/2}$, $2p_{1/2}$, and $2p_{3/2}$ levels the finite laser bandwidth and the static electric field both have a profound effect on the ionization and excitation probabilities.

The equations are useful as a description of photoionization in the numerical modeling of collective effects in transient plasmas produced by multiphoton ionization of atomic hydrogen and deuterium. When modeling collective effects an array of density matrices will be needed to represent the interaction region and to allow for spatial and temporal variations of the collective electric field.

ACKNOWLEDGMENTS

We are indebted to Dr. Martin Dörr for performing Floquet calculations and for providing helpful comments on a draft of this paper. This work has been supported under the Scientific Research Programme and the International Collaboration Programme of Enterprise Ireland. One of the authors (BJS) gratefully acknowledges receipt of a studentship from the National University of Ireland, Maynooth.

REFERENCES

1. Zoller, P., 1979, *Phys. Rev. A*, **19**, 1151.
2. Bowe, P., Giammanco, F., O'Neill, R.W., van der Burgt, P.J.M., and Slevin, J.A., 1998, *Phys. Rev. A*, **58**, 1389.
3. Giammanco, F., 1989, *Phys. Rev. A*, **40**, 5171.
4. Holt, C.R., Raymer, M.G., and Reinhardt, W.P., 1983, *Phys. Rev. A*, **27**, 2971.
5. Dörr, M., Latinne, O., and Joachain, C.J., 1997, *Phys. Rev. A*, **55**, 3697.
6. Georges, A.T. and Lambropoulos, P., 1980, *Adv. Electron. Electron Phys.*, **54**, 191.
7. Agostini, P., Georges, A.T., Wheatley, S.E., Lambropoulos, P., and Levenson, M.D., 1978, *J. Phys. B*, **11**, 1733.
8. Zoller, P. and Lambropoulos, P., 1980, *J. Phys. B*, **13**, 69.
9. Shore, B.W., 1990, *Theory of Coherent Atomic Excitation* (New York: Wiley).
10. Dai, B. and Lambropoulos, P., 1986, *Phys. Rev. A*, **34**, 3954.
11. Dörr, M., 2000, private communication.
12. Potvliege, R.M., 1998, *Comput. Phys. Commun.*, **114**, 42.
13. Latinne, O., Kylstra, N.J., Dörr, M., Terao-Dunseath, M., Joachain, C.J., Burke, P.G., and Noble, C.J., 1995, *Phys. Rev. Lett.*, **74**, 46.